



Published in final edited form as:

ACS Nano. 2017 January 24; 11(1): 946–952. doi:10.1021/acsnano.6b07537.

Crosslinked Polymer-Stabilized Nanocomposites for the Treatment of Bacterial Biofilms

Ryan F. Landis^{†,‡}, Akash Gupta^{†,‡}, Yi-Wei Lee[†], Li-Sheng Wang[†], Bianka Golba^{†,‡}, Brice Couillaud^{†,||}, Roxane Ridolfo^{†,§}, Riddha Das[†], and Vincent M. Rotello^{*,†}

[†]Department of Chemistry, University of Massachusetts Amherst, 710 North Pleasant Street, Amherst, Massachusetts 01003, United States

[‡]Department of Chemistry, Boğaziçi University, Bebek, Istanbul, Turkey, 34342

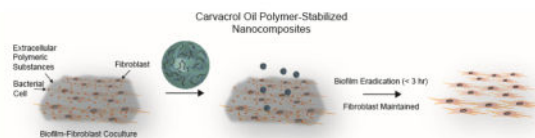
^{||}Department of Chemistry, University of Pierre and Marie Curie Paris 6, 4 Place Jussieu, Paris, France, 75005

[§]Department of Polymer Science, Colloids and Formulation, ENSCBP – Bordeaux INP, 16 Avenue Pey Berland, Pessac, France 33607

Abstract

Infections caused by bacterial biofilms are an emerging threat to human health. Conventional antibiotic therapies are ineffective against biofilms due to poor penetration of the extracellular polymeric substance (EPS) secreted by colonized bacteria, coupled with the rapidly growing number of antibiotic-resistant strains. Essential oils are promising natural antimicrobial agents, however poor solubility in biological conditions limits their applications against bacteria in both dispersed (planktonic) and biofilm settings. We report here an oil-in-water crosslinked polymeric nanocomposite (~250 nm) incorporating carvacrol oil that penetrates and eradicates multidrug-resistant (MDR) biofilms. The therapeutic potential of these materials against challenging wound biofilm infections was demonstrated through specific killing of bacteria in a mammalian cell - biofilm co-culture wound model.

Graphical Abstract



*rotello@chem.umass.edu.

[‡]R.F.L and A.G. contributed equally to the work

Conflict of Interest: The authors declare no competing financial interest.

Supporting Information Available: Shelf life of the crosslinked nanocomposites, serum stability of non-crosslinked NCs, synthesis of PONI-GAT, zeta potential/ATR-FTIR of the nanocomposites, fluorecamine – PONI-GAT calibration curve, and bacterial strain information table.

Keywords

Multidrug-resistant bacteria; biofilms; phytochemicals; crosslinked; nanocomposite

Multidrug-resistant (MDR) bacterial infections are a rapidly emerging health challenge.¹ MDR bacterial infections are responsible for 700,000 deaths each year world-wide, with more than 10 million predicted deaths per year by 2050.² A key threat is provided by biofilm infections³ of wounds and indwelling systems such as catheters,⁴ joint prosthesis,⁵ and other medical implants.⁶ Biofilms secrete extracellular polymeric substance⁷ (EPS), acting as a protective barrier against antibiotics and limiting the efficacy of drugs including vancomycin,⁸ teicoplanin,⁹ and colistin¹⁰ deemed as, “drugs of last resort”. Excising infected tissues/implants¹¹ and long-term antibiotic therapy¹² are currently the best treatments for combatting biofilm-based infections but these invasive approaches have obvious limitations, including patient suffering and inconvenience and extensive health care costs.¹³

Phytochemical^{14,15} extracts from plants are responsible for their self-defense against microbial agents,¹⁶ making them promising tools to combat MDR bacteria.¹⁷ These essential oils are of particular interest as “green” antimicrobial agents¹⁸ due to their low cost,¹⁹ biocompatibility,^{20,21} and potential anti-biofilm properties.²² Previous studies have demonstrated that many essential oils are cytotoxic towards pathogenic bacteria,^{23,24} however poor solubility²⁵ and stability²⁶ in aqueous media has substantially limited their therapeutic application. Essential oils can be encapsulated into surfactant-²⁷ and nanoparticle-stabilized²⁸ colloidal delivery vehicles to enhance their aqueous stability and antimicrobial activity against bacteria with applications in food and beverage industries.²⁹ However, these carriers can be colloidally unstable,³⁰ significantly impairing practical use, particularly in complex media such as serum.

We hypothesized that using a polymer-stabilized essential oil platform would enable us to generate nano-sized emulsions to improve the delivery of the payload,³¹ and to increase its stability³² by incorporating crosslinking strategies. Herein, we report an essential oil-in-water crosslinked polymer nanocomposite (X-NC) for the treatment of bacterial biofilms (Scheme 1). These nanocomposites exhibit high stability in storage (Supporting Information Figure S1) and serum, and rapidly penetrate into biofilms as evidenced by confocal experiments. Most importantly, X-NCs efficiently eradicate multiple pathogenic biofilms including methicillin-resistant *Staphylococcus aureus* (MRSA). The therapeutic potential of this system demonstrated using a fibroblast-biofilm co-culture wound infection model that demonstrated essentially complete elimination of bacteria while maintaining high fibroblast cell viability.

Results and Discussion

Generation and Characterization of Nanocomposites

Poly(oxanorborneneimide) polymers (PONIs) were used to stabilize and crosslink the essential oil nanocomposites, providing a well-controlled,³³ easily modulated,³⁴ and scalable

platform.³⁵ PONI was designed using three components. First, incorporating amines onto PONI would enable fast reactions with crosslinkable electrophiles loaded into the oil core as PONI approaches the oil interface. The commercially available poly(maleic anhydride-*alt*-octadecene (**p-MA-*alt*-OD**) was chosen as the electrophile to ensure effective crosslinking.³⁶ Second, guanidinium moieties were added to enable binding with bacterial membranes³⁷ along with charge neutralization with the carboxylates released from the anhydrides,³⁸ enabling PONIs to partition further into the oil phase for further amidation reactions. Finally, tetraethylene glycol monomethyl ether (**TEG-ME**) groups can impart further amphiphilicity, ensuring PONIs are water-soluble yet can partition into the oil. Therefore, we synthesized a copolymer PONI bearing guanidine, amine, and TEG-ME units (**PONI-GAT**) at a 35-35-30 monomer ratio respectively (Supporting Information – Synthesis of PONI-GAT).

PONI-GAT, carvacrol oil and **p-MA-*alt*-OD** were used to generate antimicrobial nanocomposites. Nanocomposites were created by emulsifying carvacrol oil loaded with **p-MA-*alt*-OD** or carvacrol only (non-crosslinked control) into water adjusted to a pH of 10 containing **PONI-GAT** (The pH was adjusted to ensure nucleophilicity of the amines on **PONI-GAT**). Upon emulsification, **PONI-GAT** partitions to the oil-water interface to initially stabilize the carvacrol oil droplets and with **p-MA-*alt*-OD** present, crosslinking further stabilizes the oil droplets in water. Multiple formulations of **PONI-GAT** and **p-MA-*alt*-OD** were tried to generate the smallest and most stable formulation. With a final **PONI-GAT** concentration of 6 μM and 10 wt% of **p-MA-*alt*-OD**, nanocomposites (10 wt% X-NCs) of $\sim 250\text{nm}$ were generated, as shown by transmission electron microscopy (TEM) and dynamic light scatter (DLS). Furthermore, the surface charge of nanocomposites was determined by zeta potential studies (Supporting Information S4) showing an overall negative charge resulting from the crosslinking reaction between amines and anhydrides, generating carboxylates and imparting negative charge at the oil-water interface.

Further characterization of the generated emulsions was performed with confocal microscopy. We hypothesized that reacting **PONI-GAT** with **p-MA-*alt*-OD** would change its inherent hydrophobicity and enhance its partitioning within the oil. To test this hypothesis, tetramethylrhodamine-5-isothiocyanate (TRITC, red fluorescence) was conjugated to **PONI-GAT** while 3,3-Dioctadecyloxycarbocyanine (DiO, green fluorescence) was loaded within the oil. In addition, the formulation was modulated to generate micron-sized emulsions so that confocal experiments could be performed. As shown in Figure 1a, both green and red fluorescence was co-localized within the oil, indicating a composite morphology.

After characterizing the physical properties of the nanocomposite, chemical properties within the composite structure were characterized using FTIR and fluorescamine assays. Attenuated total reflectance Fourier transform infrared spectroscopy (ATR-FTIR) indicated complete loss of anhydrides and formation of amides/carboxylates after nanocomposite fabrication (Supporting Information S5). To further explore the crosslinking, a fluorescamine assay³⁹ (Figure 1b) was performed to identify the progression of the reaction between amines on **PONI-GAT** and the anhydrides on **p-MA-*alt*-OD**.⁴⁰ **PONI-GAT** was used to generate a calibration curve relating to the polymer concentration and the respective fluorescence generated from the assay (Supporting Information S6). We expected that as the

p-MA-alt-OD wt% increases within the oil, more amines will react, and the overall fluorescence generated from fluorescamine will decrease. The results show that a substantial reduction in amines on **PONI-GAT** occurs as **p-MA-alt-OD** wt% increases, with almost complete conversion at 10 wt%.

X-NCs Penetration into Biofilms

Effective treatment of biofilms requires penetration of antimicrobial agents into the film.⁴¹ We next probed the ability of X-NCs to penetrate into biofilms. X-NCs loaded with DiO within the oil were used to track their delivery into biofilms formed by red fluorescent protein (RFP) expressing *Escherichia coli*. As shown in Figure 2, the X-NCs diffuse into the biofilm matrix and efficiently disperse throughout the biofilm, co-localizing with the bacteria. This data supports X-NCs deliver their payload and that the oil core and nanocomposite fabrication strategy are operative for effective delivery.

Antimicrobial Activity of X-NCs Against Biofilms

Next, we investigated the therapeutic efficacy of the X-NCs against multiple Gram positive and negative biofilms. Four pathogenic bacterial strains of clinical isolates, *Pseudomonas aeruginosa* (CD-1006), *Staphylococcus aureus* (CD-489, a methicillin-resistant strain), *Escherichia coli* (CD-2), and *Enterobacter cloacae* (*E. cloacae*, CD-1412) complex were chosen to test our system. As shown in Figure 3, X-NCs were able to effectively kill bacterial cells in all four biofilms within three hours. The individual components used to generate the nanocomposites were used as controls and they showed minimal toxicity to biofilms indicating that the combination of all components to generate X-NCs is critical for maximum therapeutic efficiency. Notably, X-NCs are able to effectively treat both Gram negative (*E. coli*, *P. aeruginosa*, and *E. cloacae* complex) and Gram positive (*S. aureus*) bacteria, demonstrating the broad spectrum activity of X-NCs.

Eradication of Biofilms in a Co-culture Model

Treatment of bacterial infections on human tissues and organs is even more challenging and relevant for medical applications. Biofilm infections associated with wounds and indwelling implants interfere with the host's ability to regenerate damaged tissue.⁴² In particular, fibroblasts play an important role during wound healing by aiding to close the area and rebuild necessary extracellular matrix within the skin.⁴³ We used an *in vitro* co-culture model comprised of mammalian fibroblasts cells with a biofilm grown over them. *P. aeruginosa* bacteria were seeded with a confluent NIH 3T3 fibroblast cell monolayer overnight to generate biofilms prior to X-NCs treatment. The co-cultures were treated with X-NCs for three hours, washed, and the viabilities of both bacteria and fibroblasts were determined. As shown in Figure 4, X-NCs effectively treated the biofilm infection while 3T3 fibroblast viability was largely unaffected. A four-fold log reduction (~99.5%) in biofilm colonies was obtained at 15 v/v% of X-NC emulsion.

Serum Stability of X-NCs

Nanoemulsion stability in serum media is critical for its application both topically and systemically.^{44,45,46,47} Negatively charged serum proteins can bind onto delivery vehicles,

forming a corona which can significantly alter their biological identity.^{48,49} Our crosslinked nanocomposite vehicle which bears a negatively charged surface should be resistant to serum protein adsorption. X-NCs were incubated with 10% serum media for two days and analyzed using DLS. As shown in Figure 5a, 10 wt% X-NCs showed stability with no evidence of destabilization/aggregation. As a control, non-crosslinked analogs using the same formulation minus p-MA-alt-OD showed no stability in serum (Supporting Information – S2). In addition, DiO was loaded into both crosslinked nanocomposites and non-crosslinked analogs and incubated in serum for one hour. Destabilization of the non-crosslinked analog would result in leakage and quenched fluorescence of the loaded dye.⁵⁰ Figure 5b shows that DiO maintains its fluorescence within the X-NCs while its non-crosslinked analog shows no fluorescence, further supporting the stability of X-NCs in serum conditions.

Conclusion

In summary, we report the fabrication of a polymer-stabilized oil-in-water nanocomposite that demonstrates high therapeutic activity towards pathogenic biofilms. These nanocomposites show good stability in serum and can effectively penetrate throughout biofilms. Furthermore, specific elimination of a biofilm infection while maintaining fibroblast viability in an *in vitro* co-culture was observed. The polymer-based crosslinked essential oil-in-water nanoemulsion strategy we present is a promising antimicrobial platform, opening new applications to treat wound biofilms and other biofilm-based infections. Given the limited capabilities of current topical therapeutics, we envision these nanocomposites as powerful new tools for skin-associated infections. Going further, the efficacy and modularity of this system will enable the use of essential oil-based composites as antimicrobial additives for foods and beverages. Finally, due to their unique mechanism of action, these stabilized essential oil emulsions can provide a long-term solution to the ever increasing danger of antibiotic resistance.

Materials and Methods

All reagents and materials were purchased from Fisher Scientific and used as received. NIH-3T3 cells (ATCC CRL-1658) were purchased from ATCC. Dulbecco's Modified Eagle's Medium (DMEM) (DMEM; ATCC 30-2002) and fetal bovine serum (Fisher Scientific, SH3007103) were used in cell culture. Pierce LDH Cytotoxicity Assay Kit was purchased from Fisher Scientific.

Synthesis of PONI-GAT

Synthesis can be found under Supporting Information – Synthesis of PONI-GAT.

Preparation of Nanocomposites

Stock nanocomposite solutions were prepared in 0.6 ml Eppendorf tubes. To prepare the stock X-NC emulsions, 3 μ L of carvacrol oil (containing 10 wt% p-MA-alt-OD) was added to 497 μ L of Milli-Q H₂O (previously adjusted to a pH of 10) containing 6 μ M of PONI-GAT and emulsified in an amalgamator for 50 s. The non-crosslinked analogs were done in

the same fashion however without p-MA-alt-OD dissolved in carvacrol. The emulsions were allowed to rest overnight prior to use.

Fluorescamine Assay

The fluorescamine calibration curve was generated by mixing various concentrations of PONI-GAT with fluorescamine (dissolved in acetonitrile – 2.5 mg/ml, 50 μ L aliquots) in phosphate buffer (PB – 5mM, pH = 7.4). The solutions were sonicated in the dark for 5 min, diluted with ethanol and their emission maxima at 470 nm analyzed. The percentage of amines remaining within the X-NCs at different wt% of p-MA-alt-OD was performed by diluting the stock emulsion solution by half. Afterwards, 450 μ L of PB was added along with 50 μ L of fluorescamine. The solutions were sonicated in the dark for 5 min, diluted with ethanol and their emission maxima at 470 nm analyzed.

Biofilm Formation

Bacteria were inoculated in LB broth at 37°C until stationary phase. The cultures were then harvested by centrifugation and washed with 0.85% sodium chloride solution three times. Concentrations of resuspended bacterial solution were determined by optical density measured at 600 nm. Seeding solutions were then made in M9 to reach OD₆₀₀ of 0.1. 100 μ L of the seeding solutions were added to each well of the microplate. M9 medium without bacteria was used as a negative control. The plates were covered and incubated at room temperature under static conditions for a desired period. Planktonic bacteria were removed by washing with PB saline three times.

Varied v/v % of X-NCs, made in M9 medium, were incubated with the biofilms for 3 h. Biofilms were washed with phosphate buffer saline (PBS) three times and viability was determined using an Alamar Blue assay. M9 medium without bacteria was used as a negative control.

Biofilm – 3T3 Fibroblast Cell Co-culture

Fibroblast-3T3 coculture was performed using the previously reported protocol.²⁸ A total of 20,000 NIH 3T3 (ATCC CRL-1658) cells were cultured in Dulbecco's modified Eagle medium (DMEM; ATCC 30-2002) with 10% bovine calf serum and 1% antibiotics at 37°C in a humidified atmosphere of 5% CO₂. Cells were kept for 24 hours to reach a confluent monolayer. Bacteria (*P. aeruginosa*) were inoculated and harvested as mentioned above. Afterwards, seeding solutions 10⁸ cells/ml were inoculated in buffered DMEM supplemented with glucose. Old medium was removed from 3T3 cells followed by addition of 100 μ L of seeding solution. The co-cultures were then stored in a box humidified with damp paper towels at 37°C overnight without shaking.

Nanocomposites and other control solutions were diluted in DMEM media prior to use to obtain desired testing concentrations. Old media was removed from co-culture and replaced with freshly prepared testing solutions and was incubated for 3 hours at 37°C. Co-cultures were then analyzed using a LDH cytotoxicity assay to determine mammalian cell viability using manufacturer's instructions.⁵¹ To determine the bacteria viability in biofilms, the testing solutions were removed and co-cultures were washed with PBS. Fresh PBS was then

added to disperse remaining bacteria from biofilms in co-culture by sonication for 20 min and mixing with pipet. The solutions containing dispersed bacteria were then plated onto agar plates and colony forming units were counted after incubation at 37°C overnight.

Supplementary Material

Refer to Web version on PubMed Central for supplementary material.

Acknowledgments

The support of the NIH (GM077173) is gratefully acknowledged. Clinical samples obtained from the Cooley Dickinson Hospital Microbiology Laboratory (Northampton, MA) were kindly provided by Dr. Margaret Riley.

References

1. Gupta A, Landis RF, Rotello VM. Nanoparticle-Based Antimicrobials: Surface Functionality is Critical. *F1000Res*. 2016; 5:F1000. Faculty Rev-364.
2. Tackling Drug-Resistant Infections Globally: Final Report and Recommendations. 2016 May 19. Retrieved November 05, 2016, from <https://amr-review.org/Publications>
3. Bjarnsholt T. The Role of Bacterial Biofilms in Chronic Infections. *APMIS*. 2013; 121:1–58. [PubMed: 23030626]
4. Trautner BW, Darouiche RO. Role of Biofilm in Catheter-Associated Urinary Tract Infection. *Am J Infect Control*. 2004; 32:177–183. [PubMed: 15153930]
5. Song Z, Borgwardt L, Hoiby N, Wu H, Sorensen TS, Borgwardt A. Prosthesis Infections After Orthopedic Joint Replacement: The Possible Role of Bacterial Biofilms. *Orthop Rev (Pavia)*. 2013; 5:65–71. [PubMed: 23888204]
6. Veerachamy S, Yarlagadda T, Manivasagam G, Yarlagadda PK. Bacterial Adherence and Biofilm Formation on Medical Implants: A Review. *P I Mech Eng H*. 2014; 228:1083–1099.
7. Kostakioti M, Hadjifrangiskou M, Hultgren SJ. Bacterial Biofilms: Development, Dispersal, and Therapeutic Strategies in the Dawn of the Postantibiotic Era. *Cold Spring Harb Perspect Med*. 2013; 3:a010306. [PubMed: 23545571]
8. Boneca IG, Chiosis G. Vancomycin Resistance: Occurrence, Mechanisms and Strategies to Combat it. *Expert Opin Ther Targets*. 2003; 7:311–328. [PubMed: 12783569]
9. Boger DL. Vancomycin, Teicoplanin, and Ramoplanin: Synthetic and Mechanistic Studies. *Med Res Rev*. 2001; 21:356–381. [PubMed: 11579438]
10. Dafopoulou K, Xavier BB, Hotterbeekx A, Janssens L, Lammens C, De E, Goossens H, Tsakris A, Malhotra-Kumar S, Pournaras S. Colistin-resistant *Acinetobacter Baumannii* Clinical Strains with Deficient Biofilm Formation. *Antimicrob Agents Chemother*. 2016; 60:1892–1895.
11. Kujath P, Kujath C. Complicated Skin, Skin Structure and Soft Tissue Infections - Are We Threatened by Multi-resistant Pathogens? *Eur J Med Res*. 2010; 15:544–553. [PubMed: 21163729]
12. Wu H, Moser C, Wang HZ, Hoiby N, Song ZJ. Strategies for Combating Bacterial Biofilm Infections. In *J Oral Sci*. 2015; 7:1–7.
13. Lynch AS, Robertson GT. Bacterial and Fungal Biofilm Infections. *Annu Rev Med*. 2008; 59:415–428. [PubMed: 17937586]
14. Wang H, Khor TO, Shu L, Su Z, Fuentes F, Lee JH, Kong ANT. Plants Against Cancer: A Review on Natural Phytochemicals in Preventing and Treating Cancers and Their Druggability. *Anticancer Agents Med Chem*. 2012; 12:1281–1305. [PubMed: 22583408]
15. Farzaei MH, Bahramsoltani R, Abbasabadi Z, Rahimi R. A Comprehensive Review on Phytochemical and Pharmacological Aspects of *Elaeagnus Angustifolia* L. *J Pharm Pharmacol*. 2015; 67:1467–1480. [PubMed: 26076872]
16. Hintz T, Matthews KK, Di R. The Use of Plant Antimicrobial Compounds for Food Preservation. *Biomed Res Int*. 2015; 2015:246264. [PubMed: 26539472]

17. Kon KV, Rai MK. Plant Essential Oils and Their Constituents in Coping with Multidrug-resistant Bacteria. *Expert Rev Anti-Infect Ther.* 2012; 10:775–790. [PubMed: 22943401]
18. Vergis J, Gokulakrishnan P, Agarwal RK, Kumar A. Essential Oils as Natural Food Antimicrobial Agents: A Review. *Crit Rev Food Sci Nutr.* 2015; 55:1320–1383. [PubMed: 24915323]
19. Maia MF, Moore SJ. Plant-Based Insect Repellents: A Review of Their Efficacy, Development and Testing. *Malar J.* 2011; 10:S11. [PubMed: 21411012]
20. Freire Rocha Caldas G, Araujo AV, Albuquerque GS, da Silva-Neto JC, Costa-Silva JH, de Menezes IR, Leite AC, da Costa JG, Wanderley AG. Repeated-doses Toxicity Study of the Essential Oil of *Hyptis Martiusii* Benth. (Lamiaceae) in Swiss Mice. *Evid Based Complement Alternat Med.* 2013; 2013:856168. [PubMed: 24151521]
21. Johnson S, Boren K. Topical and Oral Administration of Essential Oils – Safety Issues. *Aromatopia.* 2013; 22:43–48.
22. Saviuc CM, Drumea V, Olariu L, Chifiriuc MC, Bezirtzoglou E, Lazar V. Essential Oils with Microbicidal and Antibiofilm Activity. *Curr Pharm Biotechnol.* 2015; 16:137–151. [PubMed: 25594290]
23. Sharifi-Rad J, Sharifi-Rad M, Hoseini-Alfatemi SM, Iriti M. Composition, Cytotoxic and Antimicrobial Activities of *Satureja Intermedia* C.A. Mey Essential Oil. *Int J Mol Sci.* 2015; 16:17812–17825. [PubMed: 26247936]
24. Hosseinkhani F, Jabalameli F, Banar M, Abdellahi N, Taherikalani M, van Leeuwen WB, Emaneini M. Monoterpene Isolated from the Essential Oil of *Trachyspermum Ammi* Is Cytotoxic to Multidrug-resistant *Pseudomonas Aeruginosa* and *Staphylococcus Aureus* Strains. *Rev Soc Bras Med Trop.* 2016; 49:172–176. [PubMed: 27192585]
25. Samperio C, Boyer R, Eigel WN 3rd, Holland KW, McKinney JS, O’Keefe SF, Smith R, Marcy JE. Enhancement of Plant Essential Oils’ Aqueous Solubility and Stability Using Alpha and Beta Cyclodextrin. *J Agric Food Chem.* 2010; 58:12950–12956. [PubMed: 21077682]
26. Turek C, Stintzing FC. Stability of Essential Oils: A Review. *Compr Rev Food Sci Food Saf.* 2013; 12:40–53.
27. Chang Y, McLandsborough L, McClements DJ. Fabrication, Stability and Efficacy of Dual-component Antimicrobial Nanoemulsions: Essential Oil (Thyme Oil) and Cationic Surfactant (Lauric Arginate). *Food Chem.* 2015; 172:298–304. [PubMed: 25442557]
28. Duncan B, Li X, Landis RF, Kim ST, Gupta A, Wang LS, Ramanathan R, Tang R, Boerth JA, Rotello VM. Nanoparticle-Stabilized Capsules for the Treatment of Bacterial Biofilms. *ACS Nano.* 2015; 9:7775–7782. [PubMed: 26083534]
29. Amaral DMF, Bhargava K. Essential Oil Nanoemulsions and Food Applications. *Adv Food Technol Nutr Sci Open J.* 2015; 1:84–87.
30. Ziani K, Chang Y, McLandsborough L, McClements DJ. Influence of Surfactant Charge on Antimicrobial Efficacy of Surfactant-Stabilized Thyme Oil Nanoemulsions. *J Agric Food Chem.* 2011; 59:6247–6255. [PubMed: 21520914]
31. Akhtar J, Siddiqui HH, Fareed S, Badruddeen, Khalid M, Aqil M. Nanoemulsion: For Improved Oral Delivery of Repaglinide. *Drug Deliv.* 2016; 23:2026–2034. [PubMed: 27187792]
32. Zeeb B, Gibis M, Fischer L, Weiss J. Influence of Interfacial Properties on Ostwald Ripening in Crosslinked Multilayered Oil-in-water Emulsions. *J Colloid Interface Sci.* 2012; 387:65–73. [PubMed: 22958854]
33. Al-Badri ZM, Tew GN. Well-defined Acetylene-Functionalized Oxanorbornene Polymers and Block Copolymers. *Macromolecules.* 2008; 41:4173–4179.
34. Lin CC, Ki CS, Shih H. Thiol-norbornene Photo-click Hydrogels for Tissue Engineering Applications. *J Appl Polym Sci.* 2015; 132:41563. [PubMed: 25558088]
35. Cole JP, Lessard JJ, Lyon CK, Tuten BT, Berda EB. Intra-chain Radical Chemistry as a Route to Poly(Norbornene Imide) Single-chain Nanoparticles: Structural Considerations and the Role of Adventitious Oxygen. *Polym Chem.* 2015; 6:5555–5559.
36. Duncan B, Landis RF, Jerri HA, Normand V, Benczedi D, Ouali L, Rotello VM. Hybrid Organic-inorganic Colloidal Composite ‘sponges’ *via* Internal Crosslinking. *Small.* 2015; 11:1302–1309. [PubMed: 25381874]

37. Zhou Z, Zheng A, Zhong J. Interactions of Biocidal Guanidine Hydrochloride Polymer Analogs with Model Membranes: A Comparative Biophysical Study. *Acta Biochim Biophys Sin (Shanghai)*. 2011; 43:729–737. [PubMed: 21807631]
38. Pantos A, Tsogas I, Paleos CM. Guanidinium Group: A Versatile Moiety Inducing Transport and Multicompartmentalization in Complementary Membranes. *Biochim Biophys Acta*. 2008; 1778:811–823. [PubMed: 18178146]
39. O'Reilly E, Lanza J. Fluorescamine: A Rapid and Inexpensive Method for Measuring Total Amino Acids in Nectars. *Ecology*. 1995; 76:2656–2660.
40. Udenfriend S, Stein S, Bohlen P, Dairman W, Leimgruber W, Weigele M. Fluorescamine: A Reagent for Assay of Amino Acids, Peptides, Proteins, and Primary Amines in the Picomole Range. *Science*. 1972; 178:871–872. [PubMed: 5085985]
41. Wang LS, Gupta A, Rotello VM. Nanomaterials for the Treatment of Bacterial Biofilms. *ACS Infect Dis*. 2015; 2:3–4. [PubMed: 27622944]
42. Roy S, Elgharably H, Sinha M, Ganesh K, Chaney S, Mann E, Miller C, Khanna S, Bergdall VK, Powell HM, Cook CH, Gordillo GM, Wozniak DJ, Sen CK. Mixed-species Biofilm Compromises Wound Healing by Disrupting Epidermal Barrier Function. *J Pathol*. 2014; 233:331–343. [PubMed: 24771509]
43. Sun BK, Saprashvili Z, Khavari PA. Advances in Skin Grafting and Treatment of Cutaneous Wounds. *Science*. 2014; 346:941–945. [PubMed: 25414301]
44. Sanchez-Moreno P, Buzon P, Boulaiz H, Peula-Garcia JM, Ortega-Vinuesa JL, Luque I, Salvati A, Marchal JA. Balancing the Effect of Corona on Therapeutic Efficacy and Macrophage Uptake of Lipid Nanocapsules. *Biomaterials*. 2015; 61:266–278. [PubMed: 26005765]
45. Sanchez-Moreno P, Ortega-Vinuesa JL, Martin-Rodriguez A, Boulaiz H, Marchal-Corrales JA, Peula-Garcia JM. Characterization of Different Functionalized Lipidic Nanocapsules as Potential Drug Carriers. *Int J Mol Sci*. 2012; 13:2405–2424. [PubMed: 22408461]
46. Baran A, Flisiak I, Jaroszewicz J, Swiderska M. Serum Adiponectin and Leptin Levels in Psoriatic Patients According to Topical Treatment. *J Dermatolog Treat*. 2015; 26:134–138. [PubMed: 24754531]
47. Berthold N, Czihal P, Fritsche S, Sauer U, Schiffer G, Knappe D, Alber G, Hoffmann R. Novel Apidaecin Ib Analogs with Superior Serum Stabilities for Treatment of Infections by Gram-Negative Pathogens. *Antimicrob Agents Chemother*. 2013; 57:402–409. [PubMed: 23114765]
48. Wolfram J, Yang Y, Shen J, Moten A, Chen C, Shen H, Ferrari M, Zhao Y. The Nano-plasma Interface: Implications of the Protein Corona. *Colloids Surf B Biointerfaces*. 2014; 124:17–24. [PubMed: 24656615]
49. Saha K, Rahimi M, Yazdani M, Kim ST, Moyano DF, Hou S, Das R, Mout R, Rezaee F, Mahmoudi M, Rotello VM. Regulation of Macrophage Recognition through the Interplay of Nanoparticle Surface Functionality and Protein Corona. *ACS Nano*. 2016; 10:4421–4430. [PubMed: 27040442]
50. Haugland, RP. *Handbook of Fluorescent Probes and Research Products*. Eugene, OR: Molecular Probes; 2002. Print
51. Decker T, Lohmann-Matthes ML. A Quick and Simple Method for the Quantitation of Lactate Dehydrogenase Release in Measurements of Cellular Cytotoxicity and Tumor Necrosis Factor (TNF) Activity. *J Immunol Methods*. 1988; 115:61–69. [PubMed: 3192948]

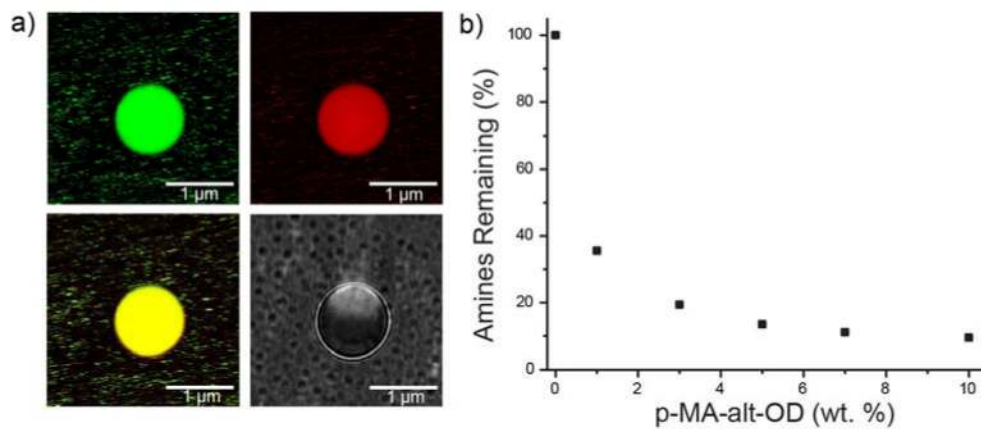


Figure 1.

Physical and chemical characterization of X-NCs. Confocal micrograph of a) crosslinked micron-sized composites. **PONI-GAT** was partially labeled with TRITC (red fluorescence) and the oil core is loaded with DiO (green fluorescence). **PONI-GAT** labeled with TRITC can be seen co-distributed with the hydrophobic core indicating a composite (as opposed to core-shell) morphology. b) Fluorescamine assay to determine the percentage of remaining amines on **PONI-GAT** after X-NCs formation.

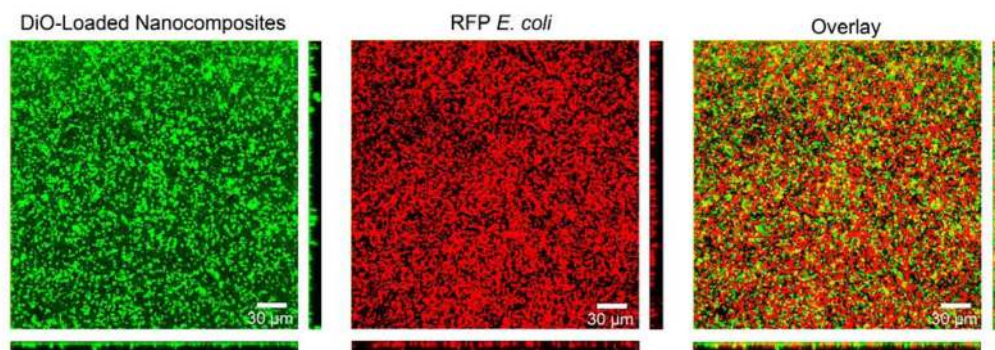


Figure 2. Confocal image stacks of *E. coli DH5a* biofilm after 3 h treatment with 10 wt% X-NCs. DiO was loaded into X-NCs to track them throughout the biofilm. The overlay shows X-NCs completely penetrate the biofilm, co-localizing with bacteria that expresses red fluorescent protein. Scale bars are 30 μm.

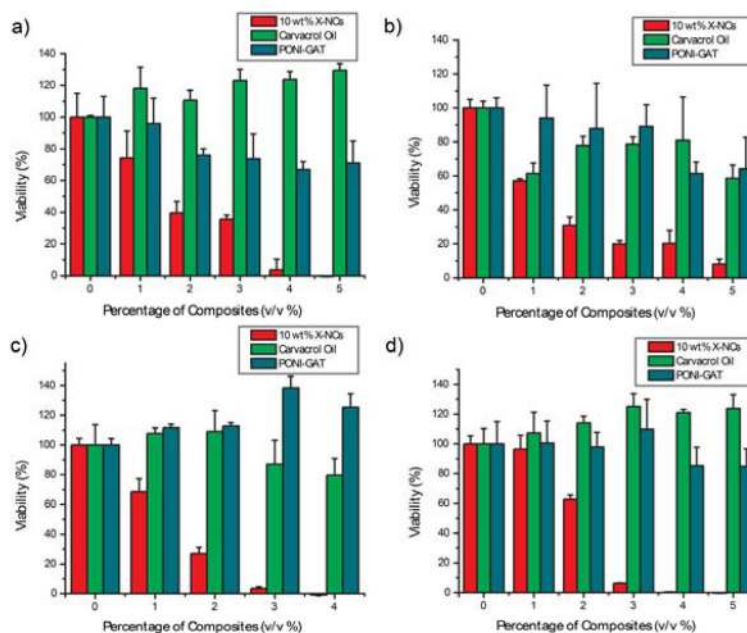


Figure 3. Viability of 1 day-old (a) *E. coli* (CD-2), (b) *S. aureus* (CD-489), (c) *P. aeruginosa* (CD-1006), and (d) *E. cloacae* complex (CD-1412) biofilms after 3 h treatment with 10 wt% X-NCs, carvacrol oil, and **PONI-GAT** at different emulsion concentrations (v/v % of emulsion). The results are an average of triplicates, and the error bars indicate the standard deviation.

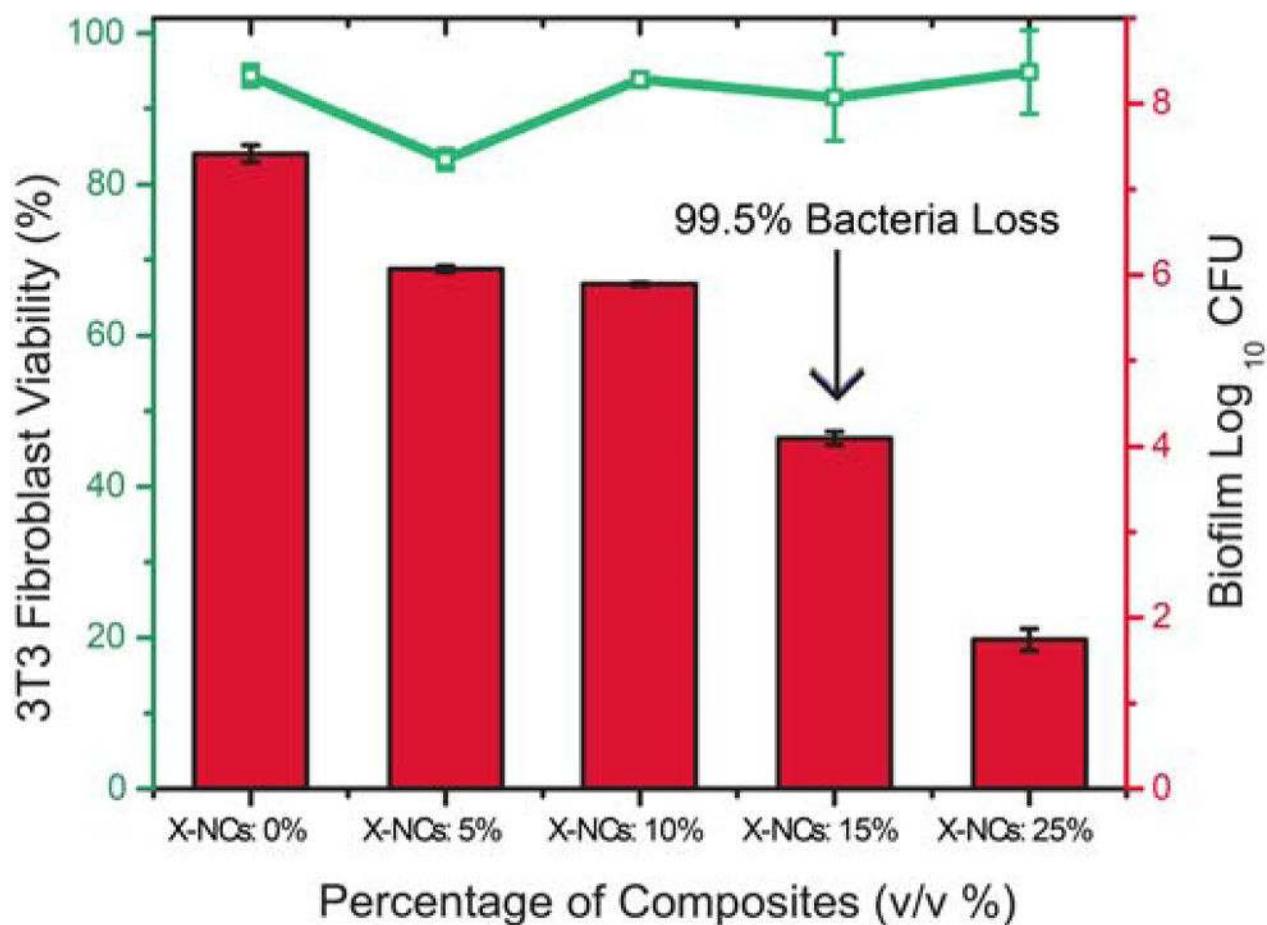


Figure 4.

Viability of 3T3 fibroblast cells and *P. aeruginosa* biofilms in the fibroblast-biofilm co-culture model after 3 h treatment with 10 wt% X-NCs at different emulsion concentrations (v/v % of emulsion). Scatters and lines represent 3T3 fibroblast cell viability. Bars represent log₁₀ of colony forming units in biofilms. The results are an average of three runs and the error bars indicate the standard deviations.

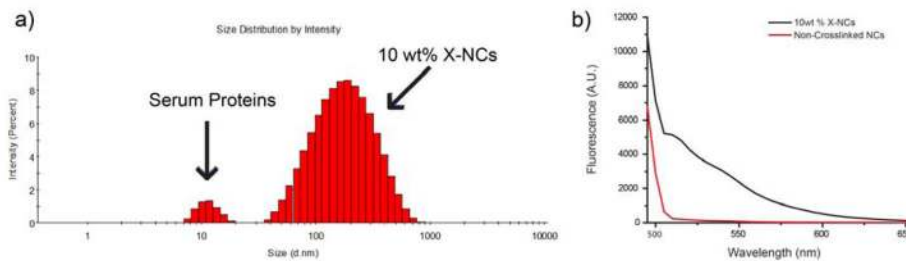
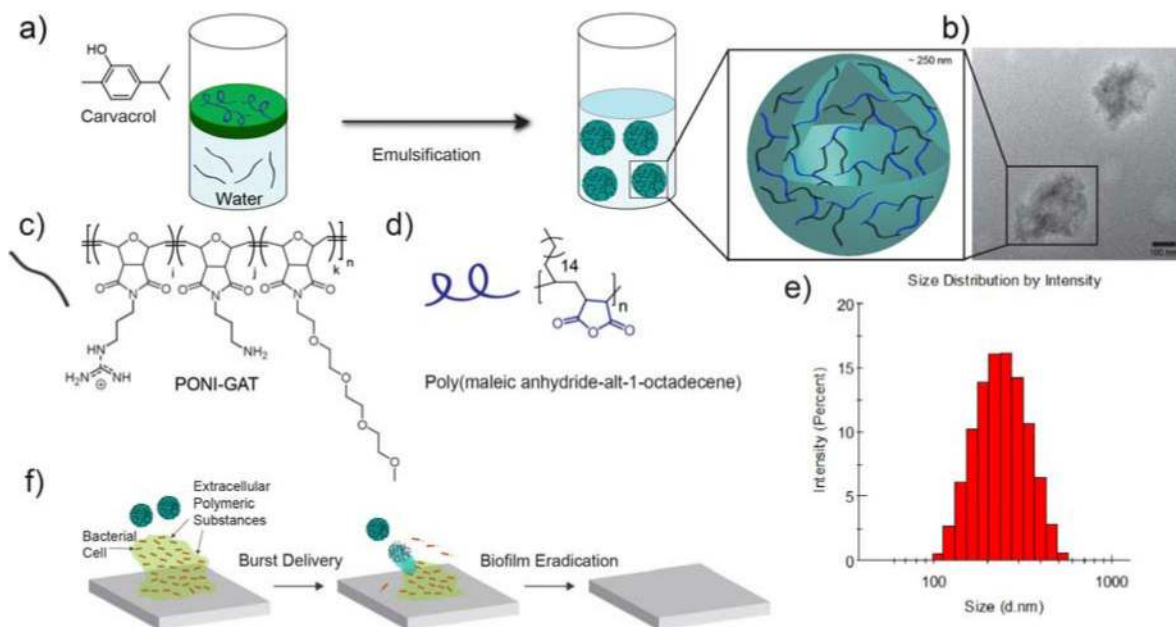


Figure 5. Stability of X-NCs in 10% fetal bovine serum (FBS). a) DLS histogram of 10 wt% X-NCs in 10% FBS after two days. Destabilization/aggregation of the X-NCs was not observed. b) Fluorescence spectra of loaded DiO in 10 wt% X-NCs and non-crosslinked analog. Serum proteins destabilizes the non-crosslinked analog, leaking out DiO, and quenching the fluorescence whereas X-NCs maintain fluorescence indicating stability. Excitation of DiO = 490nm.



Scheme 1.

Strategy used to generate antimicrobial composites a) Carvacrol oil with dissolved **p-MA-alt-OD** is emulsified with an aqueous solution containing the **PONI-GAT** polymer. The amines on **PONI-GAT** react with the anhydride units on **p-MA-alt-OD**. This crosslinking reaction simultaneously pulls **PONI-GAT** into the oil phase as the polymer becomes more hydrophobic, generating an oil-containing nanocomposite structure. b) TEM micrograph of X-NCs. Scalebar is 100 nm. c) Chemical structure of **PONI-GAT**. d) Chemical structure of **p-MA-alt-OD**. e) DLS histogram indicating the size distribution of X-NCs in phosphate buffer saline (150mM). f) Proposed mechanism of biofilm disruption.